Bioactive Materials 3 (2018) 341–346

Contents lists available at ScienceDirect

Bioactive Materials

journal homepage: http://www.keaipublishing.com/en/journals/bioactive-materials/

Combination types between graphene oxide and substrate affect the antibacterial activity

Jiajun Qiu [a, c], Lu Liu [a, b], Hongqin Zhu [a], Xuanyong Liu [a, *]

[a] State Key Laboratory of High Performance Ceramics and Superfine Microstructure, Shanghai Institute of Ceramics, Chinese Academy of Sciences, Shanghai, 200050, China
[b] Shanghai Normal University, Shanghai, 200234, China
[c] University of Chinese Academy of Sciences, Beijing, 100049, China

ARTICLE INFO

Article history:
Received 26 February 2018
Received in revised form
25 April 2018
Accepted 1 May 2018

Keywords:
Graphene oxide
Antibacterial
Titanium
Combination type
S. aureus

ABSTRACT

Duo to their superior physicochemical properties, graphene and its derivatives (GDs), such as graphene oxide (GO) and reduced graphene oxide (rGO), have attracted extensive research interests around the world. In recent years, antibacterial activities of GDs have aroused wide concern and substantial works have been done. However, the underlying antibacterial mechanisms still remain controversial. Antibacterial activities of GDs vary with various factors, such as size, number of layers, oxygen-containing groups, and experimental surroundings. We assume that combination types between graphene oxide and substrate may affect the antibacterial activity. Therefore, in this work, GO was fixed on the titanium surface with three kinds of combination types including drop with gravitational effects (GO-D), electrostatic interaction (GO-APS) and electrophoretic deposition (GO-EPD), and the antibacterial activities *in vitro* were systematically investigated. Results showed that combination types affected the ability of GO for preventing *Staphylococcus aureus* (*S. aureus*) from gathering, sharpness of wrinkles or edges and reactive oxygen spices (ROS) levels. Once *S. aureus* are in the form of separation without aggregation, GO can effectively interact with them and kill them with sharp wrinkles or edges and high ROS levels. GO-EPD could effectively prevent *S. aureus* from gathering, own sharp wrinkles or edges and could generate higher ROS levels. As a result, GO-EPD exhibited optimal antibacterial activity against *S. aureus*, followed by GO-APS and GO-D.

1. Introduction

Graphene, a sheet of two-dimensional single layer carbon atoms with sp^2 hybridized, has attracted extensive research interests around the world in recent years [1–6], duo to its superior physicochemical properties, including excellent thermal conductivity [7], high carrier mobility at room temperature [8], high Young's modulus [9], large specific surface area [10] and so on. With the exceptional properties, graphene and its derivatives (GDs), such as graphene oxide (GO) and reduced graphene oxide (rGO), are widely used in the fields of supercapacitors [11,12], fuel cells [13,14], photocatalysis [15,16] and biomedicine [17–20] and so on.

In recent years, antibacterial activities of GDs have aroused wide concern and substantial works have been done [21–23]. Currently, several predominant antibacterial mechanisms have been proposed, such as nanoknives, oxidative stress, and wrapping or trapping. However, the underlying antibacterial mechanisms still remain controversial [23]. Physicochemical properties of GDs, such as size, shape and surface functionality might affect their antibacterial activities. Lateral size of GDs can influence their adsorption ability and the amount of corners and sharp edges, which are important to the interactions between GDs and bacteria [24]. Liu et al. [25] reported that GO sheets with larger sizes exhibited stronger antibacterial activity against *E. coli* than those of smaller sizes. Number of layers of GDs can also influence the antibacterial activity. Increasing the number of layers of GDs can increase the thickness of GDs, which in turn weaken the nanoknives effect. At the same time, Increasing the number of layers of GDs can lead to agglomeration, which will reduce the chance of contact between

* Corresponding author.
E-mail address: xyliu@mail.sic.ac.cn (X. Liu).
Peer review under responsibility of KeAi Communications Co., Ltd.

https://doi.org/10.1016/j.bioactmat.2018.05.001

GDs and bacteria [23]. The existence of oxygen-containing groups can also alter the antibacterial activities of GDs by affecting the nanoknives effect and amphipathy. Akhavan et al. [26] found that rGO shown inhibition of cell proliferation of *E. coli* while GO was biocompatible with *E. coli*.

GDs mentioned above were almost dispersed in the solution. However, GDs, dispersed in the solution or fixed on the substrate surface, may exhibit different antibacterial activities. In our previous studies [27], we found that increasing the number of layers of GO on titanium surfaces could improve the antibacterial activity by increasing the reactive oxygen spices (ROS) levels which was opposite to the result as mentioned above. Moreover, we also found that GO on titanium surface presented stronger antibacterial activity than rGO which were reduced by vacuum heat treatment, hydrazine hydrate and sodium borohydride, respectively [28]. From above we can know that antibacterial activities of GDs vary with various factors, such as size, number of layers, oxygen-containing groups, experimental surroundings. Based on this, we wonder whether combination types between GO and substrate affect the antibacterial activity or not. To figure it out, in this work, GO fixed on the titanium surfaces with three kinds of combination types were fabricated and the antibacterial activities *in vitro* were systematically investigated.

2. Materials and methods

2.1. Sample preparation

Commercial pure titanium plates with the dimensions of $10 \times 10 \times 1\ mm^3$ were polished with series abrasive papers to a mirror plane on one side of the titanium plates, which were denoted as Ti. Samples with different combination types between GO and titanium substrate were fabricated as follows. With gravitational effects, 100 μL of single layer GO aqueous solution (0.06 mg/mL, purchased from Hangzhou Gaoxi Technology Co., Ltd) was dropped on the Ti surface, dried in the air and denoted as GO-D. To adhere GO on the titanium surface with electrostatic interaction, Ti was immersed in NaOH aqueous solution (5 M) for 12 h to obtain Ti-OH on titanium surfaces, and then reacted with 5% of 3-animopropyl-trimethoxysilane (APS) for 2 h with continuous ultrasonic to get amino (NH_2) on titanium surfaces. Finally, GO was adhered to the titanium surfaces via electrostatic interaction between GO and amino with impregnation method, and the corresponding samples were denoted as GO-APS. A combination type different from GO-D and GO-APS was achieved on titanium surface with cathode electrophoresis deposition (EPD). To be more specific, GO, absorbed with metal cation (Zn^{2+}) which made GO positively charged, was deposited on titanium surface with cathode EPD and the corresponding samples were denoted as GO-EPD.

2.2. Surface characterization

Field-emission scanning electron microscope (FE-SEM, Magellan 400, FEI, USA) with an accelerating voltage of 2 KV was used to observe the surface morphologies of Ti, GO-D, GO-APS and GO-EPD. Chemical compositions of various samples were determined with X-ray photoelectron spectroscopy (XPS, PHI 5300) with an Mg K_α source (250 W, 14 KV). Raman spectra on various sample surfaces were obtained by Raman microscope system (LabRAM, Horiba Jobin Yvon, France) with an excitation wavelength at 514 nm using an Ar-ion laser. X-ray diffraction (XRD, D8 discover, Bruker) using Cu Kα as the radiation source with 1° glancing angle was applied to investigate the phase compositions on the titanium surfaces.

2.3. In vitro antibacterial experiments

2.3.1. SEM observation

Gram-positive *Staphylococcus aureus* (*S. aureus*) (ATCC 25923) was used to assess the antibacterial activities of Ti, GO-D, GO-APS and GO-EPD. To clearly observe the morphology and integrity of cell membrane, SEM observation was performed as follows. First, Ti, GO-D, GO-APS and GO-EPD were sterilized with 75% (v/v) ethanol for 2 h and dried in the super clean bench. Subsequently, bacterial suspensions (60 μL, 10^7 CFU/mL) were seeded on various sample surfaces and cultured at 37 °C for 24 h. After culturing for 24 h, the bacteria on sample surfaces were fixed with 2.5% glutaraldehyde solution overnight, dehydrated in gradient ethanol solution (30, 50, 75, 90, 95 and 100% (v/v)) and dried in hexamethyl disilazane ethanol solution series. Finally, the images were taken using SEM (S-3400 N, Hitachi, Japan) with an accelerating voltage of 15 KV.

2.3.2. Agar culture observation

Antibacterial activities of Ti, GO-D, GO-APS and GO-EPD were further assessed with agar culture. For agar culture, after culturing for 24 h at 37 °C, the samples with bacterial suspensions were transferred into test tubes with 4 mL of 0.9% NaCl solution and shook to detach the bacteria from the samples. And then, bacterial suspensions were serially diluted with 0.9% NaCl solution in tenfold steps. At last, 100 μL of diluted bacterial suspensions were introduced to a standard agar culture plate (Tryptic Soy Broth for *S. aureus*) for further cultivation with 24 h at 37 °C. Finally, photographs of agar culture plates were taken.

2.3.3. Bacterial viability assessment

Bacterial viability assessment of Ti, GO-D, GO-APS and GO-EPD was performed with alamarblue assay kit. After culturing for 24 h at 37 °C, 500 μL of 10% alamarblue was added into each sample and cultured for another 2 h at 37 °C. Finally, 100 μL medium was transferred to a 96-well black plate and the corresponding fluorescent intensity (FI) was detected with an excitation wavelength at 560 nm and an emission wavelength at 590 nm. The antibacterial ratio was calculated as follows,

$$\text{Antibacterial ratio}\ (\%) = \frac{FI_{control} - FI_{experiment}}{FI_{control}} \times 100$$

Where $FI_{control}$ was the fluorescent intensity of control group, $FI_{experiment}$ was the fluorescent intensity of experiment group.

2.4. Agar diffusion assay

To figure out whether release of Zn ions on GO-EPD contributes to antibacterial effect, agar diffusion assay was performed on all the samples. First, 100 μL of bacterial suspensions with a density of 10^7 CFU/mL were introduced to the Trypticase Soy Broth (TSB) agar culture plates. Then, various specimens were put on TSB agar culture plates and cultured for 24 h at 37 °C. Finally, images of agar culture plates were taken.

2.5. Intracellular reactive oxide species assay

ROS levels in bacteria cells were investigated using 2′,7′-dichlorodihydrofluorescein diacetate (DCFH-DA) which can be deacetylated with intracellular esterases into nonfluorescent 2′,7′-dichloro-dihydrofluorescein (DCFH). And then, DCFH can be oxidized with ROS into fluorescent 2′,7′-dichlorofluorescein (DCF). Therefore, the fluorescent intensity of DCF presents the ROS level to some extent. To determine the intracellular ROS levels, bacteria were cultured on Ti, GO-D, GO-APS and GO-EPD for 24 h at 37 °C, and then, 500 μL of

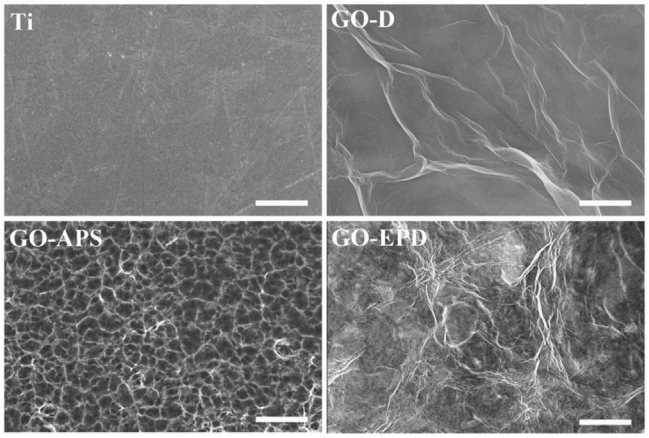

Fig. 1. Surface morphologies of Ti, GO-D, GO-APS and GO-EPD. The scale bar is 2 μm.

DCFH-DA (10 μM) was introduced to each sample and cultured for another 30 min. Eventually, 100 μL medium was transferred to a 96-well black plate and the corresponding fluorescent intensity of DCF was detected using a microplate reader with extinction wavelength of 488 nm and emission wavelength of 535 nm.

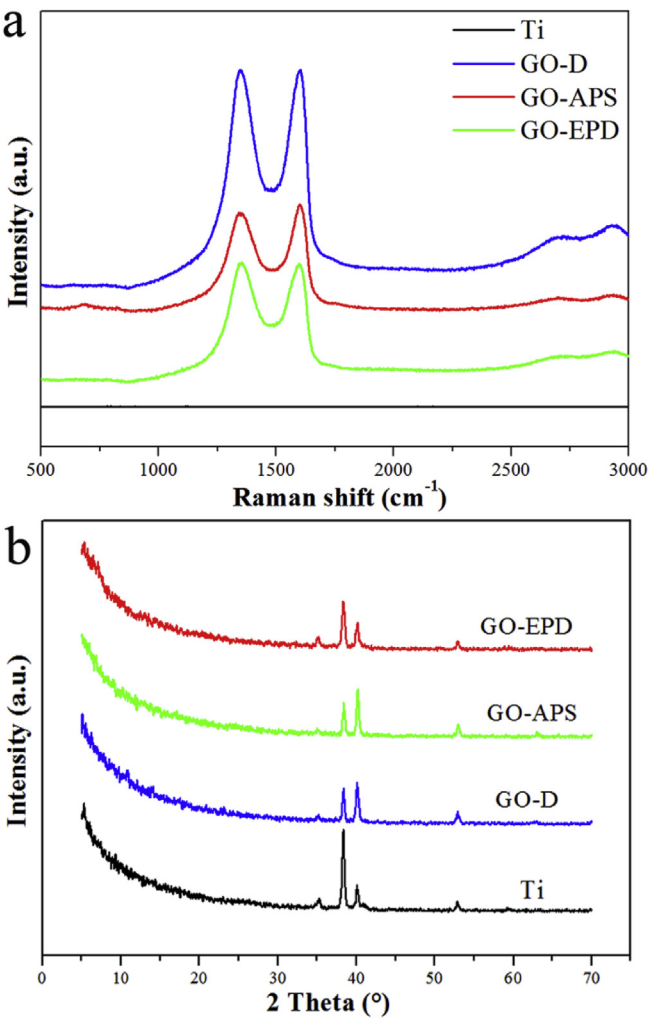

Fig. 2. (A) Raman spectra of Ti, GO-D, GO-APS and GO-EPD; (b) XRD patterns of Ti, GO-D, GO-APS and GO-EPD.

2.6. Statistical analysis

The Data were expressed as the mean ± standard deviation. Statistically significance difference was analyzed using the GraphPad Prism 5 software package. A value of $P < 0.05$ suggested statistically significant difference.

3. Results and discussion

3.1. Surface characterization

Surface morphologies of Ti, GO-D, GO-APS and GO-EPD are shown in Fig. 1. Ti had a relatively flat surface after polishing with abrasive papers in series. Large GO sheets with wrinkles could be observed on GO-D. Compared to GO-D, GO uniformly overspread on GO-APS and shown obvious fluctuation of wrinkles or edges and thinner thickness which reticulate structures on titanium surface after alkali treatment could be clearly seen. GO on GO-EPD exhibited a higher density of wrinkles or edges. From Fig. 1, we can see that wrinkles or edges of GO on GO-APS and GO-EPD are sharper than that on GO-D. Fig. 2a exhibits the raman spectra of Ti, GO-D, GO-APS and GO-EPD. Raman spectrum of Ti, without characteristic peaks, shown a straight line. For GO-D, GO-APS and GO-EPD, the typical features of GO, i.e. the D band at 1350 cm^{-1} and the G band at 1580 cm^{-1}, were detected which indicated that GO with different combination types were fixed on the titanium surface. XRD patterns of Ti, GO-D, GO-APS and GO-EPD are presented in Fig. 2b. All the samples presented the typical features of Ti. Feature peak of GO at 11° approximately was not detected on GO-D, GO-APS and GO-EPD, which suggested that GO was in the form of amorphous state with the stack of single layer GO. To investigate the chemical compositions of various samples, XPS was used and the results are shown in Fig. 3. C, O, and Ti elements were detected on Ti. With the coverage of GO on GO-D, Ti element was invisible and not detected. As mentioned above, compared to GO-D, the thickness of GO on GO-APS was thinner. Therefore, Ti element could be detected on GO-APS, though the peak intensity was weak. For GO-EPD, Ti element was also not detected with the deposition of GO on the titanium surface. As aforementioned, GO, absorbed with Zn ions which made GO positively charged, was deposited on titanium surface with cathode EPD. Therefore, Zn element also be detected on GO-EPD.

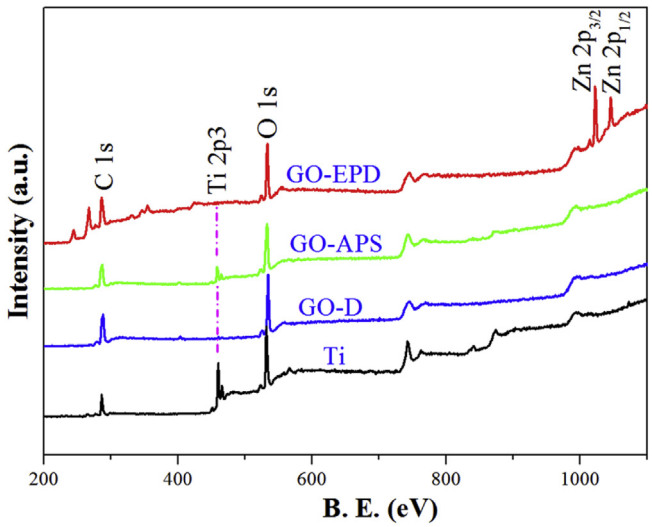

Fig. 3. XPS full spectra of Ti, GO-D, GO-APS and GO-EPD.

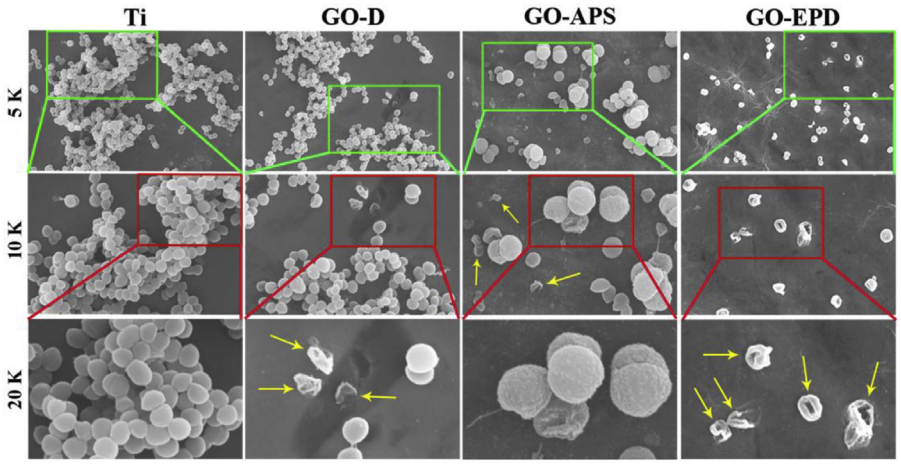

Fig. 4. SEM observation of *S. aureus* on Ti, GO-D, GO-APS and GO-EPD at different magnification.

3.2. In vitro antibacterial activity

Gram-positive *S. aureus* was used to investigate the antibacterial activity of Ti, GO-D, GO-APS and GO-EPD. Surface morphologies of *S. aureus,* after culturing for 24 h at 37 °C on various sample surfaces, are presented in Fig. 4. At low magnification of 5 K and 10 K, a lot of bacteria gathered and adhered on the titanium surface. From the high magnification of 20 K, it could be clearly seen that *S. aureus* grew well on Ti with the typical features of smooth, round and intact cell morphology. For GO-D, plenty of bacteria could also

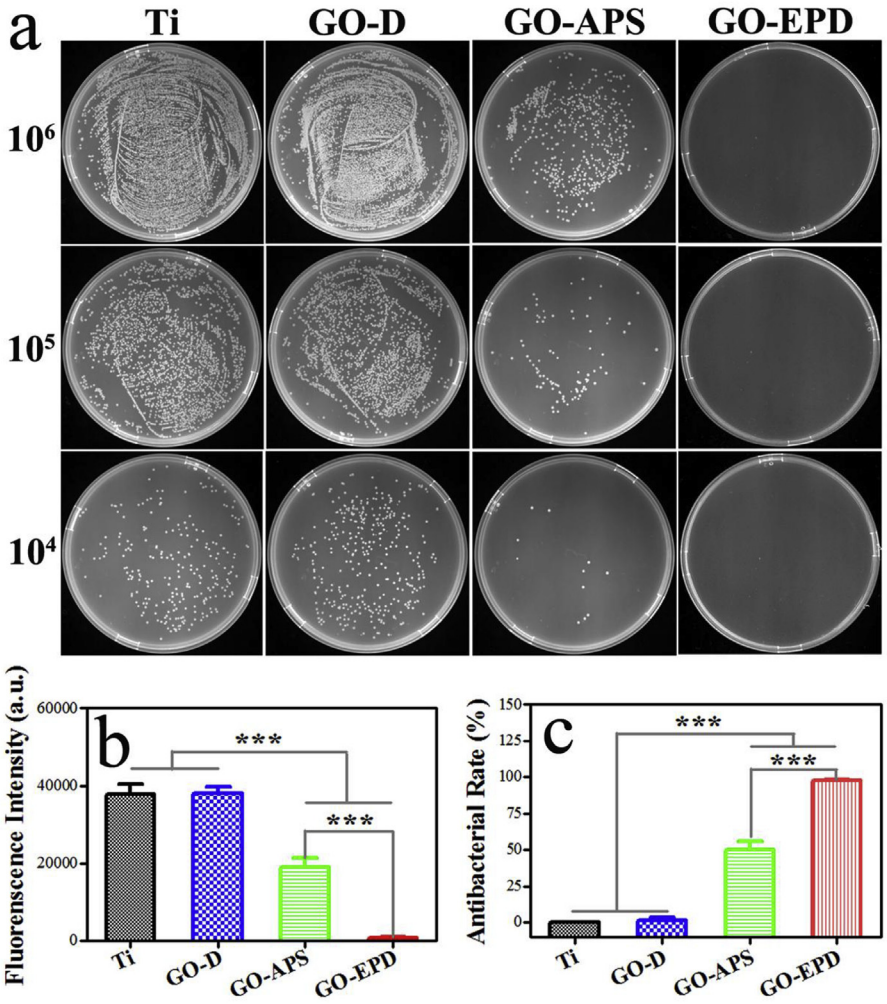

Fig. 5. (A) Bacterial colonies of re-cultivated *S. aureus* on agar culture plates; (b) bacterial viability of *S. aureus* on Ti, GO-D, GO-APS and GO-EPD and (c) corresponding antibacterial rate.

be found and gathered on the sample surface from the low magnification of 5 K. However, at the high magnification of 10 K and 20 K, we found that a small amount of bacteria in the form of separation without aggregation were dead with severely deformed cell membrane as shown in yellow arrows. As for GO-APS, compared to Ti, fewer amount of bacteria adhered on the sample surface and there existed two kinds of bacteria, which one exhibited small size in the form of separation, another one had large size in the form of aggregation. From the high magnification of 10 K and 20 K, we could clearly see that bacteria in the form of separation with small size were dead with the cell membrane badly damaged as shown in yellow arrows, while bacteria in the form of aggregation with large size had a very rough surface though the cell membrane was relatively intact. Among all the samples, the amount of bacteria on GO-EPD was the least. Interestingly, bacteria on GO-EPD were almost in the form of separation and totally dead with the most badly distortion of cell membrane as shown in yellow arrows.

To further investigate the antibacterial activity, agar culture and bacteria viability were performed. For agar culture, 60 μL of bacterial suspensions with the density of 10^7 CFU/mL were seeded on Ti, GO-D, GO-APS and GO-EPD and cultured for 24 h at 37 °C, and then the bacteria were collected, diluted and re-cultured on the agar culture plates for another 24 h. As shown in Fig. 5a, a lot of bacterial colonies could be found on Ti at the density of 10^6 CFU/mL. Compared to Ti, the amount of bacterial colonies on GO-D had no significant difference, while the number of bacterial colonies on GO-APS significantly reduced. Moreover, bacterial colonies on GO-EPD were almost invisible. After diluting in series, the trend could be more clearly recognized that GO-EPD had the best antibacterial activity, followed by GO-APS.

For bacterial viability, after culturing for 24 h at 37 °C, 500 μL of 10% alamarblue was added and cultured for another 2 h. Finally, 100 μL medium was transferred to a 96-well black plate and the fluorescent intensity was detected and the corresponding antibacterial rate was calculated. Results are presented in Fig. 5(b and c). GO-EPD exhibited the lowest bacterial viability ($p < 0.001$ vs Ti, GO-D, and GO-APS), followed by GO-APS ($P < 0.001$vs Ti and GO-D). Bacterial viability between GO-D and Ti had no significant difference. Antibacterial rates of various samples were calculated based on the bacterial viability which GO-EPD presented the best antibacterial activity with the antibacterial rate of almost 100%, followed by GO-APS with the antibacterial rate of 49.8%. GO-D had no significantly antibacterial effect compared with Ti.

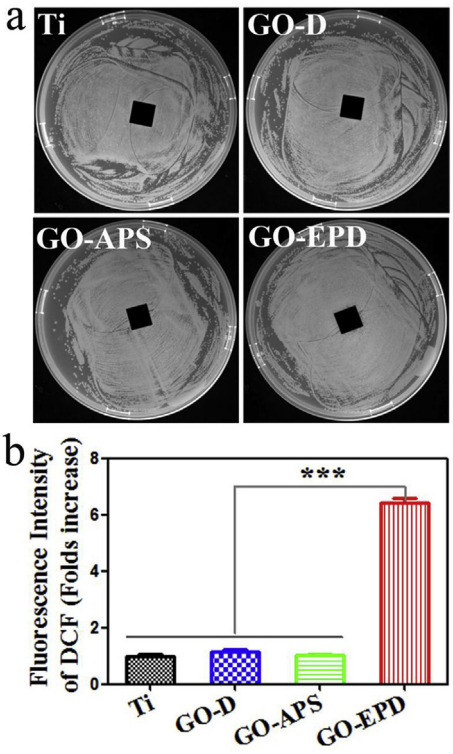

Fig. 6. (A) Inhibition zones around various samples against *S. aureus*; (b) fluorescence intensity of DCF on various samples.

To figure out whether release of Zn ions makes a contribution to the antibacterial activity of GO-EPD, agar diffusion assay was performed on all the samples and the results are shown in Fig. 6a. No inhibition zones around the samples could be found from Ti, GO-D, GO-APS and GO-EPD which indicated that Zn ions herein had nothing to do with the antibacterial activity. At the same time, ROS levels in bacteria cells were investigated and the results are presented in Fig. 6b. GO-EPD exhibited higher ROS level ($P < 0.001$ vs. Ti, GO-D and GO-APS). ROS levels among Ti, GO-D and GO-APS had no significant difference.

From above, we find that combination types affect the ability of GO for preventing *S. aureus* from gathering. The ability for preventing *S. aureus* from gathering of all the samples as shown in Fig. 4 meets the following relation: GO-EPD > GO-APS > GO-D. Once *S. aureus* are in the form of separation without communication with each other, GO can effectively interact with them. From Fig. 1, we can see that wrinkles or edges of GO on GO-APS and GO-EPD are sharper than that on GO-D. *S. aureus* which are in the form of separation without aggregation can be easily cut by GO with sharp wrinkles or edges. Therefore, GO-APS and GO-EPD present better antibacterial activities than GO-D. Moreover, GO-EPD exhibited higher ROS level. Therefore, GO-EPD presented optimal antibacterial activity, followed by GO-APS.

4. Conclusions

In this work, GO was fixed on the titanium surface with three kinds of combination types including drop with gravitational effects, electrostatic interaction and electrophoretic deposition. The antibacterial activities of GO with different combination types with titanium substrates *in vitro* were systematically investigated. Results showed that combination types could influence the ability of GO for preventing *S. aureus* from gathering, sharpness of wrinkle or edges and reactive oxygen spices levels. Once *S. aureus* are in the form of separation without aggregation, GO can effectively interact with them and kill them with sharp wrinkles or edges and high reactive oxygen spices levels. GO-EPD could effectively prevent *S. aureus* from gathering, own sharp wrinkles or edges and could generate higher ROS levels. Therefore, GO-EPD presented optimal antibacterial activity, followed by GO-APS and GO-D.

Acknowledgements

Financial support from the National Key Research and Development Program of China (2016YFC1100604), the National Science Foundation for Distinguished Young Scholars of China (51525207), National Natural Science Foundation of China (31670980, 31570973), Shanghai Committee of Science and Technology, China (17441904000, 15441904900) are acknowledged.

References

[1] C. Chung, Y.K. Kim, D. Shin, S.R. Ryoo, B.H. Hong, D.H. Min, Biomedical applications of graphene and graphene Oxide, Acc. Chem. Res. 46 (10) (2013) 2211–2224.

[2] X. Huang, Z.Y. Zeng, Z.X. Fan, J.Q. Liu, H. Zhang, Graphene-based electrodes, Adv. Mater. 24 (45) (2012) 5979–6004.
[3] V. Singh, D. Joung, L. Zhai, S. Das, S.I. Khondaker, S. Seal, Graphene based materials: past, present and future, Prog. Mater. Sci. 56 (8) (2011) 1178–1271.
[4] Y.W. Zhu, S. Murali, W.W. Cai, X.S. Li, J.W. Suk, J.R. Potts, R.S. Ruoff, Graphene and graphene oxide: synthesis, properties, and applications, Adv. Mater. 22 (35) (2010) 3906–3924.
[5] J.S. Wu, W. Pisula, K. Mullen, Graphenes as potential material for electronics, Chem. Rev. 107 (3) (2007) 718–747.
[6] Y.Q. Sun, Q.O. Wu, G.Q. Shi, Graphene based new energy materials, Energy Environ. Sci. 4 (4) (2011) 1113–1132.
[7] A.A. Balandin, S. Ghosh, W.Z. Bao, I. Calizo, D. Teweldebrhan, F. Miao, C.N. Lau, Superior thermal conductivity of single-layer graphene, Nano Lett. 8 (3) (2008) 902–907.
[8] K.S. Novoselov, A.K. Geim, S.V. Morozov, D. Jiang, Y. Zhang, S.V. Dubonos, I.V. Grigorieva, A.A. Firsov, Electric field effect in atomically thin carbon films, Science 306 (5696) (2004) 666–669.
[9] C. Lee, X.D. Wei, J.W. Kysar, J. Hone, Measurement of the elastic properties and intrinsic strength of monolayer graphene, Science 321 (5887) (2008) 385–388.
[10] M.D. Stoller, S.J. Park, Y.W. Zhu, J.H. An, R.S. Ruoff, Graphene-based ultracapacitors, Nano Lett. 8 (10) (2008) 3498–3502.
[11] Y.P. Zhang, H.B. Li, L.K. Pan, T. Lu, Z. Sun, Capacitive behavior of graphene-ZnO composite film for supercapacitors, J. Electroanal. Chem. 634 (1) (2009) 68–71.
[12] F.H. Li, J.F. Song, H.F. Yang, S.Y. Gan, Q.X. Zhang, D.X. Han, A. Ivaska, L. Niu, One-step synthesis of graphene/SnO2 nanocomposites and its application in electrochemical supercapacitors, Nanotechnology 20 (45) (2009).
[13] Y.M. Li, L.H. Tang, J.H. Li, Preparation and electrochemical performance for methanol oxidation of Pt/graphene nanocomposites, Electrochem. Commun. 11 (4) (2009) 846–849.
[14] L.F. Dong, R.R.S. Gari, Z. Li, M.M. Craig, S.F. Hou, Graphene-supported platinum and platinum-ruthenium nanoparticles with high electrocatalytic activity for methanol and ethanol oxidation, Carbon 48 (3) (2010) 781–787.
[15] H.T. Liu, S.M. Ryu, Z.Y. Chen, M.L. Steigerwald, C. Nuckolls, L.E. Brus, Photochemical reactivity of graphene, J. Am. Chem. Soc. 131 (47) (2009) 17099–17101.
[16] H. Zhang, X.J. Lv, Y.M. Li, Y. Wang, J.H. Li, P25-graphene composite as a high performance photocatalyst, ACS Nano 4 (1) (2010) 380–386.
[17] S.Y. Wu, S.S.A. An, J. Hulme, Current applications of graphene oxide in nanomedicine, Int. J. Nanomed. 10 (2015) 9–24.
[18] N. Li, Y.L. Cheng, Q. Song, Z.Y. Jiang, M.L. Tang, G.S. Cheng, Graphene meets biology, Chin. Sci. Bull. 59 (13) (2014) 1341–1354.
[19] O. Akhavan, Graphene scaffolds in progressive nanotechnology/stem cell-based tissue engineering of the nervous system, J. Mater. Chem. B 4 (19) (2016) 3169–3190.
[20] H.M. Hegab, A. ElMekawy, L.D. Zou, D. Mulcahy, C.P. Saint, M. Ginic-Markovic, The controversial antibacterial activity of graphene-based materials, Carbon 105 (2016) 362–376.
[21] J. Tang, Q. Chen, L.G. Xu, S. Zhang, L.Z. Feng, L. Cheng, H. Xu, Z. Liu, R. Peng, Graphene oxide-silver nanocomposite as a highly effective antibacterial agent with species-specific mechanisms, ACS Appl. Mater. Interfaces 5 (9) (2013) 3867–3874.
[22] W.B. Hu, C. Peng, W.J. Luo, M. Lv, X.M. Li, D. Li, Q. Huang, C.H. Fan, Graphene-based antibacterial paper, ACS Nano 4 (7) (2010) 4317–4323.
[23] X.F. Zou, L. Zhang, Z.J. Wang, Y. Luo, Mechanisms of the antimicrobial activities of graphene materials, J. Am. Chem. Soc. 138 (7) (2016) 2064–2077.
[24] X. Cai, S.Z. Tan, M.S. Lin, A. Xie, W.J. Mai, X.J. Zhang, Z.D. Lin, T. Wu, Y.L. Liu, Synergistic antibacterial brilliant blue/reduced graphene oxide/quaternary phosphonium salt composite with excellent water solubility and specific targeting capability, Langmuir 27 (12) (2011) 7828–7835.
[25] S.B. Liu, M. Hu, T.H. Zeng, R. Wu, R.R. Jiang, J. Wei, L. Wang, J. Kong, Y. Chen, Lateral dimension-dependent antibacterial activity of graphene oxide sheets, Langmuir 28 (33) (2012) 12364–12372.
[26] O. Akhavan, E. Ghaderi, Escherichia coli bacteria reduce graphene oxide to bactericidal graphene in a self-limiting manner, Carbon 50 (5) (2012) 1853–1860.
[27] J.J. Qiu, H. Geng, D.H. Wang, S. Qian, H.Q. Zhu, Y.Q. Qiao, W.H. Qian, X.Y. Liu, Layer-number dependent antibacterial and osteogenic behaviors of graphene oxide electrophoretic deposited on titanium, ACS Appl. Mater. Interfaces 9 (2017) 12253–12263.
[28] J.J. Qiu, D.H. Wang, H. Geng, J.S. Guo, S. Qian, X.Y. Liu, How oxygen-containing groups on graphene influence the antibacterial behaviors, Adv. Mater. Interfaces 4 (15) (2017).